

Chapter 2

Background

Abstract

Atmosphere-, marine-, and soil-derived chemical species are incorporated into microcrystalline ices during their normal environmental cycles. It is generally assumed that species trapped in deep ice cores would be indefinitely preserved, thereby providing a reliable record of Earth's paleoclimate. However, it has become apparent that ice contaminants are chemically transformed over geological timeframes, even under the low temperatures and apparent isolation prevalent at large depths. Of particular interest today are the apparent CO and CO₂ excesses found in Greenland ice bubbles relative to contemporaneous Antarctic records prior to ca. 1500 AD. This recently observed phenomenon requires the *in situ* oxidation or decomposition of organic material below the firn line, i.e., after air bubbles are closed off in core sections strictly blocked from solar radiation. The detection of $\mu\text{g Kg}^{-1}$ levels of dicarboxylic, oxocarboxylic, and dicarbonylic species in Greenland, but not in the cleaner Antarctic ice cores, lends material support to the hypothesis of ongoing chemical activity in deep ice cores. The nature, likelihood, mechanisms, and rates of chemical or physical processes involved in these transformations remain, however, uncharted issues.

The observed CO excesses exclude the acidification of carbonates as the sole source of CO₂. Since most organic compounds are unreactive toward closed-shell oxidizing agents such as H₂O₂ in acidic media below -30 °C, dark oxidative pathways would require catalytic action, possibly involving iron oxides from co-deposited atmospheric dust. Photochemical processes are deemed to be restricted to the top layers (< 3 m) due to radiation scattering by the high-albedo snow cover and by the underlying firn layer.

However, about $10 \text{ photons cm}^{-3} \text{ s}^{-1}$ ($\lambda > 230 \text{ nm}$) are evenly and continuously evolved by relativistic muons of cosmic origin (i.e., Cerenkov radiation) as they traverse ice cores. Recent measurements have shown that deep glacier ice is extremely transparent to UV-vis radiation between 220 and 430 nm. Photons in this spectral region would be exclusively absorbed by contaminants, specifically by the chromophores carried in by the atmospheric aerosol incorporated into the snow. It has been estimated that about $\sim 4 \times 10^{11} \text{ CO molecules cm}^{-3}$ would be formed over a millennium by photochemical decarbonylation of such chromophores with unitary quantum efficiency, an amount equivalent to the excess CO found in Greenland ice cores.

Introduction

The primary goal of this chapter is to understand the photochemical fate of dissolved organic matter trapped in ice. The information is also relevant to atmospheric chemical processes taking place in high-latitude polar environments where photochemistry occurring in near-surface snowpacks can impact the overlying atmosphere.

CO and CO₂ found in Greenland ice bubbles are found in excess relative to contemporaneous Antarctic records for the last thousand years. This discrepancy may be explained by the *in situ* decomposition of organic material in ice core sections by Cerenkov radiation. In order to support this proposal, the background information necessary to approach the problem of photochemistry in ice core records is presented, followed by a description of the physicochemical properties of ice as a reaction medium, and a discussion on the potential relevance of this mechanism to historical CO and CO₂ ice core records.

Historical Ice Core Records

Ice is an important component of the terrestrial and atmospheric environments. Seasonal or perennial ice covers large portions of the high-latitude oceans and landforms. The chemical composition of polar ices is particularly valuable to researchers because it contains paleoatmospheric and paleoclimatic imprints.¹⁻⁴ At a density of 0.8 g cm⁻³, which is reached at depths of 50 m or more, firn pores become encapsulated, trapping air that would reflect the composition of past atmospheres. It has been generally assumed that such deposits are well preserved, considering the prevalent low temperatures and the fact that sunlight is completely backscattered by snow and firn in the upper few meters.⁵⁻⁷

According to this view, photochemical activity would be restricted to the seasonal processing of snow contaminants,⁸⁻¹² a subject that has recently attracted much attention. Irradiated snow caps are apparently the source of the high levels of surface NO_x, HO_x, and aldehydes at high latitudes, including Arctic regions and the South Pole,¹³⁻³² which impact the boundary layer ozone.^{14,26,29,33}

CO and CO₂ Anomalies in Greenland Samples

The reconstruction of past atmospheric carbon dioxide concentrations based on ice core analysis may help assess the long-term impact of anthropogenic emissions on Earth's climate. Various records from Greenland and Antarctic sites representing the last 300 years are in good agreement on global pre-industrial CO₂ concentrations of about 280 ppmv. However, a recent study indicates that Greenland records predating the second millennium AD contain CO₂ excesses of about 20 ppmv over their South Pole counterparts, within sections representing a few annual layers.³⁴ The fact that formaldehyde and hydrogen peroxide concentrations' profiles are anticorrelated with those of carbon dioxide, and the observation that the CO₂ excesses become larger in older bubbles suggest the occurrence of chemical processing, possibly the oxidation of organic material, as the cause of the anomaly. A comparative study of CO levels in Greenland and Antarctica ice cores points to a similar phenomenon. CO mixing ratios in Greenland ice core air bubbles begin to exceed those of Antarctica by about 100 ppbv before ca. 1600 AD. The sudden occurrence of high CO concentrations at about 155 m depth suggests the presence of organic species, which are able to produce carbon monoxide, otherwise absent from the ice cores.^{35,36}

Possible Mechanisms of In Situ CO and CO₂ Production in Ice Cores

Considering that any modification of air composition in the firn layer would not translate into discrete features within the ice core because of convective and diffusive mixing inside the interconnected pore network, and with the atmosphere, the above observations imply measurable chemical activity at subfreezing temperatures in the complete absence of sunlight. As such, they represent a scientific challenge and undermine the key assumption of chemically inert polar ice cores. Previous claims on chemical activity in such environments were made in relation to Greenland hydrogen peroxide records,³⁷ which showed a larger number of partially depleted narrow (ca. 10 cm) layers with increasing depth.^{38,39} Atmospheric dusty conditions are generally associated with arid continental surfaces resulting from glaciations. Dust represents the insoluble fraction of atmospheric aerosol and comprises iron-oxide-bearing minerals and soot.⁴⁰ The heterogeneous catalytic decomposition of H₂O₂ on granular size goethite (α -FeOOH) actually takes place in aqueous media under various experimental conditions.⁴¹ The catalytic decomposition of hydrogen peroxide on oxide surfaces generates OH radical that could possibly initiate the oxidation of organic material accumulated at ice-bubble interfaces. It should be emphasized that only OH radicals could drive oxidation of typical ice core organic material, such as light carboxylic acids, to carbon oxides at low temperature.⁴²

However, the fact that most core sections are acidic and contain carbonates, organic material, and oxidizing agents after thousands of years demonstrates that mere reagent availability does not necessarily lead to chemical reaction. Solutes are essentially isolated

within the ice structure and would only react after an encounter, an outcome subject to concentration gradients and molecular mobilities. One of the key open questions in ice core research is whether trace species are evenly distributed or are enriched at grain boundaries or in veins. Therefore, the crucial issue regarding the possibility of thermal oxidation reactions proceeding at detectable rates is the relative distribution of oxidant, substrate, and catalyst within ice veins and grain boundaries at the onset. In contrast, photochemical transformations are in general unimolecular events. The photochemical production of carbon monoxide has actually been observed upon illumination of freshly fallen snow samples in the Alps. Initial rates of CO formation are strongly correlated with the total organic carbon content of the samples.³⁶ Thus, the photochemical generation of CO in deep ice cores would become a conceivable process if a plausible source of actinic radiation were identified.

Properties of Bulk Ice

The dielectric properties of the ice/water system are unique among polar liquids. The dielectric constant of water, ϵ , is very high and increases at lower temperature.^{43,44} Remarkably, ϵ keeps increasing in the solid, a direct indication that its dielectric properties are not associated with rotating dipoles, but with the long-range polarization of the entire lattice, probably via H-bonding chains. “Normal” liquids experience a drastic drop of the dielectric constant upon freezing.

The electrical properties of ice are also unique and may be very important in trying to understand its role as a reaction medium. Ice provides a good example of electrical conduction by protons, which have mobilities of about an order of magnitude larger than

those characteristic of normal ionic conductors. Recent work indicates that protons only become immobile below 190 K on the surface of ice.⁴⁵ In fact, many analogies can be established between protonic conduction in ice and electronic conduction in metals and intrinsic semiconductors. Ionic impurities can have drastic effects on the dielectric and conduction properties, particularly at low frequencies.

Several dynamical processes occurring in ice exhibit intriguing similarities in activation energies and rate constants, such as dielectric and elastic relaxation, self-diffusion, spin-lattice relaxation, and motion narrowing of magnetic resonance lines.⁴⁶ Interestingly, oxygen and hydrogen diffuse at the same rate, suggesting that the primary diffusing species is not an ion, but an intact water molecule.

Chemical Properties of Ice/Vapor and Ice/Water Interfaces

Ice surfaces are chemically distinct phases. Thus, although proton transfer between ammonia and hydronium



proceeds instantaneously in the aqueous phase, it never reaches equilibrium on ice surfaces due to restrictions on ion mobility.⁴⁷ The reason is that at high coverage NH_3 encounters not only H_3O^+ but also, increasingly, NH_4^+ , with which it forms ammoniated, immobile clusters.

Hydrogen chloride becomes less than 50% dissociated on ice at temperatures below 120 K. On the other hand, NaCl readily dissociates to Na^+ and Cl^- ions on a condensed

water surface, even at 100 K.⁴⁸ However, the temperature dependence of solute interactions with water-ice is so steep that it is unwarranted to extrapolate very low-temperature data to field conditions.⁴⁹

The electrical and chemical changes at the ice-solution interface during the freezing of electrolyte solutions depend on the rate of freezing. This is a complex, non-equilibrium process, which generates electrical potential and pH changes. The equilibrium electrical properties of ice/water interfaces have been investigated.⁵⁰ The reversible electrostatic potential is created by protonation equilibria involving atmospheric OH groups, and therefore is pH-dependent. The isoelectric point of ice, i.e., the conditions under which ice particles suspended in water are electrophoretically quiescent, i.e., $\zeta = 0$, was found to be close to pH = 4 using an ice electrode.⁵⁰⁻⁵² In an interesting approach, the electrophoretic mobility and zero point charge (zpc) were determined for D₂O (mp = 3.8 °C) ice particles suspended in H₂O.⁵³ In 1 mM NaCl, 3.5 °C, $\zeta = 0$ at pH = 3.0, and zpc is reached at pH = 7.0. The inference is that chloride ions are specifically adsorbed at the ice/water interface.

Freezing and Ice Polymorphs

Ice can adopt many crystalline structures, more than any other known material. At ordinary pressures the stable phase of ice is called ice I, which exists in two closely related variants: hexagonal ice (I_h), with hexagonal symmetry, and cubic ice (I_c), which has a diamond-like structure. I_h is the usual form of ice. I_c is formed by deposition at very low temperatures, below 140 K, which are beyond the environmental range. Amorphous ice can be made by depositing water vapor onto a substrate at still lower temperatures,

and therefore does not qualify either as a simile for environmental ices. Environmental ices can grow from the vapor phase, or by freezing water or aqueous solutions.⁵⁴ The properties and morphologies of the ices formed depend on nucleation and growth kinetics, which are a function of the degree of supersaturation and the presence of solutes.⁵⁵ Sparse ice aerosols may settle into polycrystalline aggregates having distinct mesoscopic characteristics.⁵⁴ The degree of crystallinity of the ice formed by vapor deposition is known to depend on the deposition rate.⁵⁶ In past studies it has been found that the phase of ice may affect the chemistry of molecules adsorbed on its surface.⁵⁷ Remarkably, heterogeneous freezing on $(\text{NH}_4)_2\text{SO}_4$ depends on its morphology.⁵⁸ If the solid is in the form of microcrystals, freezing begins at the eutectic temperature, but on large ammonium sulfate crystals heterogeneous freezing occurs at the normal melting point. Thus, ice cores, ice clouds, snow, and oceanic ice caps actually represent different reaction media.

From the viewpoint of experimental design it should be emphasized that the structure and properties of thin ice films markedly depend on the properties and morphology of the substrate, as revealed by IR spectroscopy,⁵⁹ and therefore are not, in general, valid surrogates for materials formed by unconstrained freezing, such as snow or marine ice caps.⁶⁰⁻⁶⁹ The phenomenon of interfacial premelting of ice (see below), so important from the environmental point of view since the quasi-liquid layer will be the location of most solutes, will occur when, loosely speaking, the polarizability of water lies between that of the ice and the substrate.⁷⁰ The polarizability of a material is a function of its refractive index and, therefore, results obtained in thin ice films deposited on optical materials such as Ge ($n = 4.0$) will have to be qualified regarding its transportability to environmental

ice. The novelty of the ice/water system stems from the fact that the polarizability of ice is greater than that of water at high frequencies, while at lower frequencies is smaller. The effect of retardation is to attenuate the high-frequency contributions. Thus, ice on a surface having a low-frequency polarizability larger than water will melt completely. If the third phase is water vapor, surface melting is limited to a finite thickness.^{70,71}

Sintering is an important process occurring in ice at finite rates above about -35 °C, which must be taken into account to ensure experimental reproducibility. It has been found that the radius of the neck x that forms between two ice spheres of radius r is given by the expression

$$\left(\frac{x}{r}\right)^n = \frac{A(T)}{r^m} \quad (2-2)$$

where n and m are integers, the values of which depend on the dominant mechanism by which material is transferred to the neck, and $A(T)$ is a function of temperature and mechanism.⁵⁴

A fundamental parameter in the growth of ice from the vapor phase is the condensation coefficient α_c , which is defined as the probability that an $\text{H}_2\text{O}(\text{g})$ molecule will stick to ice surfaces. Typical α_c values decrease with temperature between 0.2 °C below -90 °C, to 0.01 °C above -13 °C. The latter value approaches α_c in water near the melting point, consistent with the existence of a liquid film over ice. Mass accommodation coefficients α_c of $\text{H}_2\text{O}(\text{g})$ on water as a function of temperature were recently measured by Li et al.⁷²

The Quasi-Liquid Layer

Faraday suggested in 1859 that ice is covered by a “liquid-like” layer. The existence of such a layer does not contradict the phase rule, as it has been argued before, which in its simple form for bulk phases, $F = C + 2 - P$, states that there is only a single ($F = 0$) state (specified by two parameters P, T) in which three macroscopic phases ($P = 3$) can coexist in a one-component system ($C = 1$). In fact, the consideration of surfaces as distinct phases requires specifying an additional intensive parameter, the surface tension γ , which naturally increases the number of intensive variables. Hence, the phase rule has to be cast in the form $F = C + 3 - P$. In other words, it is thermodynamically possible to have three phases –gas, solid, and liquid film– over a range of temperatures below the normal freezing point.^{73,74}

Bulk ice is covered by a quasi-liquid layer of variable thickness down to about 240 K.^{75,76} The thickness of the liquid layer markedly depends on the presence of ice impurities.⁷⁷⁻⁷⁹ However, the onset of ice surface disordering depends on the technique used to monitor the changes.⁸⁰ The critical temperature will also vary depending on the conditions under which the experiments are performed, the presence of surface impurities, and the different nature and sensitivity of the techniques employed. For example, atomic force microscopy indicates that at temperatures below 243 K supercooled water droplets form on top of a nm ice layer in contact with a cleaved mica substrate. After annealing, a continuous flat film is formed. Between 263 and 253 K and a relative humidity of 83% the film consists of a solid ice layer about 0.7 nm thick, covered with a liquid-like layer about 5 nm thick.⁶⁶ Rejected solutes will populate such layer,

which is more akin to a fluid than to a solid medium, or accumulate into veins and nodes.^{81,82} Solute mobility in the top two or three bilayers is substantially faster than in the bulk, even at low temperatures.⁸³

Solute Rejection and Partitioning during Freezing: Solute Migration and Diffusion

Freezing at or below eutectic temperatures can create solid solutions, depending on the extent of ice-solution equilibration. It should be emphasized that a system is completely solid only below its eutectic point. In the range of temperatures between the freezing and eutectic points, ice and fluid solution coexist.⁸⁴ At the eutectic point, ice and solute may separate as independent solid phases or not, depending on their compatibility. It is always possible to reach such a condition by cooling the solutions sufficiently fast, i.e., by preventing solvent freezing at temperatures above the eutectic point.⁸⁵ In general, with a few exceptions such as NH_4F , polar, non-polar, or ionic solutes are segregated from ice upon freezing above the eutectic point.⁸⁶ The existence of solid solutions in which ice is the major component has only been demonstrated for NH_4F , HF, and a few organic acids. However, ammonium also enhances the solubility in ice of anions that do not fit easily into the ice structure.

The precise location of solutes in ice matrices remains controversial.^{87,88} Atmospheric or aerosolized marine species can be deposited on growing ice surfaces, and their local environment within the solid being formed will change as they become buried under successive layers.^{81,89-93} In the important case of clouds, it has been shown that the relationship between fresh snow and air composition will depend on the growth rate of snow crystals.⁹⁴

In most aqueous solutions studied,⁸⁷ ice grown from solution remains nearly pure. Even within the liquid layer, solute distribution within microcrystalline ice aggregates is not homogeneous, but tends to peak at the triple intersection of grain boundaries.⁹⁵ Information on the distribution of these ions, i.e., whether they are disseminated through the crystals or concentrated in a liquid phase at the triple junctions between the crystals, is essential to model these systems.⁹⁶ It has been found that liquid SO_4H_2 is concentrated at the junctions, but that NaCl and its ions could not be detected inside ice crystals. The relationship between the degree of ionization and the environment of a strong acid is also of great importance. Often this relationship reduces to the interdependence of ion/acid hydration and proton transfer. Even in the presence of pure water, the surface of crystalline ice, particularly at cryogenic temperatures, is one of limited water availability. Recent infrared spectroscopic work has found that the surface of free-standing ice particles is badly disordered, with a range of water-ring sizes and an increased level of H-bond saturation relative to an ordered ice surface. DCl and DBr are present as molecular adsorbates. HNO_3 , however, behaves differently even at 135 K.⁹⁷

There is indirect evidence on the liquid nature of the ice/air interface via SO_2 uptake on ice spheres.⁸⁹ Physical studies on the adsorption of simple, non-polar hydrocarbon vapors on ice reveal that below $-35\text{ }^\circ\text{C}$ adsorption is characterized by low adsorption energies, with isosteric heats lower than the heat of condensation at low coverage. Above that temperature, adsorption changes dramatically to that of adsorption on liquid water, implying a discontinuity in the properties of ice at $-35\text{ }^\circ\text{C}$, above which it becomes covered with a liquid film.⁹¹ The phenomenon is an equilibrium one because it is not

history-dependent, despite the fact that the total surface available for adsorption decreases at higher temperatures due to sintering.

Escape of insoluble gases out of the aggregates will take place mainly by diffusion through the lattice voids, and therefore the length of the diffusive path will depend on tortuosity, i.e., the mesoscopic structure of the ice pack. Diffusion under simultaneous concentration and temperature gradients leads to isotopic fractionation within ice pores. Post-depositional migration can certainly influence the interpretation of paleoclimatic information.^{98,99} Conflicting reports on nitric acid diffusion on ice surfaces attest to the difficulty of characterizing ice structures.^{94,100-102} Post-depositional loss of nitrate has been observed in surface snow layers of the Antarctic ice-sheet.^{103,104}

Chemical Reactions upon Freezing

Chemical reactions may take place on preformed ice or during freezing.^{84,105} The differential incorporation of ions in ice during the freezing of solutions generates transiently charged interfaces.¹⁰⁶ The extent of non-equilibrium, which depends on the rate of freezing, may induce thermodynamically forbidden reactions. It has been shown that concentration of the rejected solutes remaining in the liquid phase during freezing accounts for the acceleration of chemical rates in most cases,¹⁰⁷⁻¹¹⁰ but this is a rather trivial effect. There are remarkable findings that cannot be accommodated by concentration effects alone. A maximum at about $-15\text{ }^{\circ}\text{C}$ in the rate constant of nitrite and sulfite oxidation has been ascribed to the interplay of the increased electrolyte concentration and the lower reaction rate constant at lower temperatures.¹¹¹

In binary systems it is simple to distinguish between a true solid-state reaction and a liquid-phase process by determining whether products are still formed below the eutectic temperature. In complex multicomponent systems, as they arise in the environment, the lowest temperature at which liquid may exist is often far below the eutectic point of the major component. However, the absence of discontinuities in the dependence of the correlated overall rate constant for the kinetics of Fe(III)-Fe(II) electron transfer in 0.55 perchloric acid media above and below its eutectic point at $-55\text{ }^{\circ}\text{C}$ was interpreted as evidence against diffusion control, and in favor of electron transfer mediated by the ice matrix.¹¹² The Fe(III)/Fe(II) equilibrium is also modified by freezing.¹¹³ The effect of freezing on a variety of acidified and neutral, nitrite ion and halide-containing mixtures has been investigated. Several trihalide ions were formed, including I_2Cl^- , I_2Br^- , ICl_2^- , and IBr_2^- , and the mechanism may involve INO and the nitroacidium ion, $[\text{H}_2\text{ONO}]^+$.¹¹⁴

It should be emphasized that the above reactions are thermodynamically allowed, i.e., exclusion from the ice matrix only enhances their rates. More interesting is the finding that some endoergic reactions, such as the reduction of CO_2 to formate and formaldehyde, occur under the non-equilibrium conditions prevailing during fast freezing.¹¹⁵⁻¹¹⁸ The transient charge separation that develops at the advancing ice front provides the overpotential required to drive the otherwise uphill redox process:



for which we estimate a free energy defect $\Delta G_{2-3} > 300 \text{ kJ} \sim 3\text{V}$ under neutral conditions, $p_{\text{O}_2} = 0.21 \text{ atm}$, 300 K . Clearly, reaction 2-3 would not proceed to any detectable extent

under equilibrium conditions in homogeneous, uncharged phases. Formally, reductions will take place on ice if it were positively charged by the preferential incorporation of H^+ relative to OH^- . Finnegan et al. have argued forcibly in favor of H^+ and OH^- as the ions involved in charge separation, in dissidence with previous reports.^{87,88,119-123} One last possibility is that high pressure could trigger certain reactions above a certain threshold level. However, 130 m ice depths amount to 1 MPa, which is far below the typical pressures required to modify reactivity in solids.¹²⁴

Cerenkov Radiation

The fact that ice cores are completely shielded from sunlight¹²⁵ does not necessarily rule out photochemical transformations. The reason is that relativistic muons of cosmic origin weakly emit continuous Cerenkov radiation throughout ice cores. The faint bluish glow emitted by transparent substances in the neighborhood of strong radioactive sources is the visible manifestation of Cerenkov radiation,¹²⁶⁻¹²⁸ which is generated as the medium is perturbed by relativistic charged particles. Although particles cannot move faster than the speed of light in the vacuum, they can still exceed the speed of light in a dense medium such as ice. With a refractive index of $n \sim 1.32$ over most of the UV spectral region, the speed of light in ice is $c_{ice} = c/1.32 = 0.757 c$. Thus, charged particles moving faster than c_{ice} would induce a macroscopic polarization field about a plane moving with the particle and perpendicular to its trajectory. The reason is that the medium cannot relax fast enough to maintain instantaneous electroneutrality.¹²⁷ The resultant dipole field will be felt even at large distances from the track. The emissions will be spread over a band of frequencies corresponding to the various Fourier

components of the pulse generated by the relativistic particle. All charged particles with velocities $v = \beta c > c_{\text{ice}}$ will induce Cerenkov emissions in the medium.

The classical theory of Frank and Tamm, based on the above considerations about the origin of the Cerenkov radiation, leads to the following expression for N the number of photons emitted by the particle in the range of wavelength $[\lambda_1, \lambda_2]$ as it traverses the distance L :¹²⁷

$$N = 2\pi\gamma L \left(\frac{1}{\lambda_1} - \frac{1}{\lambda_2} \right) \left(1 - \frac{1}{\beta^2 n^2} \right) \quad (2-4)$$

where $\gamma = 1/137$ is the fine structure constant and n is the average refractive index of the medium. Muons, produced by the interaction of cosmic rays with matter, are positively charged elemental particles with a rest mass of $m_0 = 1.88 \times 10^{-28}$ Kg, i.e., about 206 times heavier than the electron. Their typical kinetic energies T exceed 1 GeV, which is much larger than the threshold energy for Cerenkov emissions in ice at about 65 MeV. From the relativistic expression for β :

$$\beta = \sqrt{1 - \frac{1}{[1 + (T / m_0 c^2)]^2}} \quad (2-5)$$

and $m_0 c^2 = 105$ MeV for the muon, we find that muons with $T > 1$ GeV, have $\beta > 0.996 > 0.757$ and are, therefore, Cerenkov active. From Equation 2-1, with $230 < \lambda/nm < 400$, $n = 1.32$, $\beta \sim 1$, we estimate that about ~ 322 photons cm^{-1} are continuously emitted along

the track of the muon. An integral flux of energetic muons ($T > 0.5$ GeV) at the sea level of about $0.04 \text{ muons cm}^{-2} \text{ s}^{-1}$ will therefore generate $0.04 \times 322 \sim 13$ actinic photons $\text{cm}^{-3} \text{ s}^{-1}$ uniformly in the ice cores. The weakly attenuated muons will travel hundreds of meters in ice before their kinetic energies drop below the Cerenkov threshold (see above). This mechanism represents a homogeneous, steady production at all depths. The estimated photon dose over a millennium amounts to $4 \times 10^{11} \text{ photons cm}^{-3} = 0.7 \text{ nMolar}$, which is in the range of chemically detectable concentrations.

Optical Properties of Deep Ice

The attenuation of sunlight through snow is due to absorption and mainly to scattering.^{11,129} The directional properties of the photon field also affect its spectral distribution as a function of depth.¹³⁰ The optical properties of snow covering the Arctic tundra were investigated⁶ showing that photosynthetically active radiation decreases nearly exponentially with depth, dropping by an order of magnitude within the first 10-20 cm. Extinction coefficients of $\alpha = 35 \text{ m}^{-1}$ and 17 m^{-1} were measured before and after melting, confirming that after the onset of melting light penetrates deeper into the snowpack. The visual albedo of the snowpack dropped from 0.75 in early June to 0 within two weeks. Light at $\lambda < 500 \text{ nm}$ is completely reflected by snow, but longer wavelengths are able to penetrate it. Above $\lambda > 1250 \text{ nm}$, the albedo drops to zero. Therefore, the photochemical transformation of snow dopants by sunlight occurs close to the snow/air interface rather than in the bulk.^{130,131} From this viewpoint, dopants become isolated from sunlight after being buried a couple of meters.

The optical properties of deep ice are very different from those of snow and firn. The absorption coefficients of bubble-free ice obtained by freezing ultra purified water in the laboratory were measured in the range 250–500 nm,¹³² and display a minimum of about 0.04 m^{-1} at about 450 nm. However, these data have been dramatically superseded by field measurements on deep ice. The optical properties of deep ice in the UV-visible range were investigated in connection with the AMANDA (Antarctic Muon and Neutrino Detector Array) experiment. The experiment involves the detection of Cerenkov radiation emitted by energetic neutrinos that penetrate the ice cap from underneath, rather than from the top, using the earth as a filter to eliminate interference from other cosmic particles. At depths of 800-1000 m, scattering is dominated by residual air bubbles, while absorption is due to the ice itself and to impurities. Photons experience a random walk from the emitter to the detectors, bouncing specularly at each ice-bubble interface, while being absorbed along the magnified path. In this way, neutrinos were actually detected via their Cerenkov emissions by sensors buried in Antarctic ice.¹⁴

From a molecular point of view, photon absorption by water-ice in the visible and near-UV is dominated by dipolar transitions involving overtones of intermolecular and intramolecular vibrations. However, the probability of higher-order multiphoton processes decays exponentially, leading to absorption coefficients smaller than 0.001 m^{-1} below 500 nm. On the other hand, the tail of the ultraviolet absorptions due to excited states of molecular water as perturbed by intermolecular interactions within the ice matrix, the so-called Urbach tail, drops steeply above 200 nm. Absorption in the intervening spectral region is largely due to atmospheric impurities incorporated into the snow and subsequently processed in the firn layer. These results are quite relevant

because they lead to intrinsic ice absorption coefficients in the photochemically useful region that are orders of magnitude smaller than previous data obtained in laboratory ice. In other words, while Cerenkov radiation shorter than 230 nm is largely absorbed by ice, near-UV photons will be exclusively absorbed by embedded contaminants.¹³³⁻¹³⁵

Peculiarities of Ice as a Reaction Medium

While field studies show that ice dopants and pollutants undergo chemical and photochemical modification, and there is a certain source of UV radiation of cosmic origin at all depths, the current understanding of the photochemical processes that may take place in ice media is rudimentary.

The early interest in the subject originated from evidence revealing that ice is a unique chemical environment. In 1957 Szent-Gyorgyi reported dramatic spectral emissive changes caused by freezing aqueous solutions of a number of dyes.¹³⁶ He found that crystalline ice is essential for the quenching of the emitting triplet state into a dark singlet ground state.¹³⁶ The results represent genuine matrix effects on electronic states and radiationless transitions in polyatomic species, and specifically rule out alternative interpretations based on enhanced solute-solute intermolecular interactions via concentration effects from solute rejection by the freezing solution.^{84,105} Concentration effects cause electron magnetic resonance (EMR) line broadening upon slow freezing. The removal of the responsible solute-solute intermolecular interactions is partially achieved by rapid freezing and requires glass-forming additives.¹³⁷ These observations highlight the crucial role of the freezing protocol in the experiment outcome.

Related results have shown that, whereas thymine undergoes photodimerization in frozen aqueous solutions, the dimer dissociates upon continuous irradiation of the thawed solutions.^{129,136} Some chemical reactions take an entirely different course in ice: The addition of Cl₂ to propene yields 1,2-dichloropropane, rather than 2-chloro-1-propanol, the dominant product in water.¹³⁸

The Chemical Identity of Organic and Inorganic Chromophores in Ice Cores

Colored organic matter found in ice cores derives from the water-soluble component of atmospheric aerosol. However, there is very little information on its chemical functionalities. Short chain carboxylic and dicarboxylic acids, as well as complex organic compounds were reported.¹³⁹⁻¹⁴¹ Humic acid, i.e., the brown material consisting of multifunctional oxygenated organic compounds has been found in the aerosol.¹⁴² A homologous series of α,ω -dicarboxylic acids (C₂-C₁₀), among other species such as oxoacids and dicarbonyls, were determined in Greenland ice core samples (206 m deep, 450 years old).^{92,93,143} This study identified succinic acid as the most abundant species, with a mean concentration of 4.8 ng g⁻¹. Much less organic material is found in Antarctic ice, due to its remoteness from continental landmasses. The fact that oxalic, rather than succinic, is the most abundant diacid in the atmosphere¹⁴⁴ clearly suggests post-depositional processing in ice cores. The photoinduced atmospheric oxidation of unsaturated fatty acids is expected to be initiated at the site of unsaturation. For example, the photochemical oxidation of oleic (9-octadecenoic) acid in snow and ice is the plausible source of azelaic acid (C9).¹⁴³ It should be emphasized that saturated carboxylic acids are resistant to oxidation by atmospheric O₃.¹⁴⁵ The recent characterization of polar

organic compounds in fog water by liquid chromatography with UV diode array and mass spectrometry detection revealed that most of the UV active organic compounds in fog water are largely acidic and polyfunctional. The acidic organic components absorb between 200 and 450 nm.^{142,146,147} A simplified model of the water-soluble organic component of atmospheric aerosols includes neutral compounds such as dialkyl ketones (16%), acids such as alkanedioic acids (15%), hydroxyalkanoic acids (15%), and polycarboxylic acids such as fulvic acid (41%).¹⁴⁷

Since carbonylic compounds can enolize and/or hydrate in aqueous media, and considering that light absorption by carbonyl functionalities extends above 300 nm, whereas *gem*-diols are transparent down to 230 nm, it is very important to establish the actual form of carbonylic species in the quasi-liquid layer. The thermodynamics of the exothermic carbonyl hydration in aqueous solutions favors hydration at lower temperatures,¹⁴⁸ but the solutes rejected into the quasi-liquid layer will find limited water availability. Solid-state ¹H NMR of frozen solutions is a suitable technique to elucidate this crucial phenomenon.

For example, it was found that UV absorption by aqueous biacetyl corresponds to about 25% of the dicarbonyl form, the remaining being due to the monocarbonylic species resulting from partial hydration:¹⁴⁹



The degree of hydration of the carbonyl group of glyoxylic acid C(O)HC(O)OH (pK_a = 3.3) markedly depends on the ionization state. The longest wavelength absorption of

the glyoxylate anion is centered at 357 nm, indicative of substantial carbonyl character. However, undissociated glyoxilic acid does not absorb above 275 nm.¹⁵⁰ Thus, the temperature dependence of the pK_a's of the α -oxocarboxylic acids will also affect the extent of hydration of the carbonyl group.

Some inorganic species can absorb solar actinic radiation within ice cores, such as O₃, H₂O₂, NO₂, HONO, HONO₂, NO₂⁻, and NO₃⁻.¹⁵¹ At 340 nm, their respective optical absorption coefficients are ϵ (base 10, L mole⁻¹ cm⁻¹): 2.0, 0.11, 359, 45, < 0.005, 17, and < 0.9. repectively. However, their photochemical contributions could be substantially larger under the short wavelength Cerenkov radiation ($\lambda > 230$ nm) transmitted through glacial ice.

Photochemistry of Natural Organic Matter and its Photodegradation Products

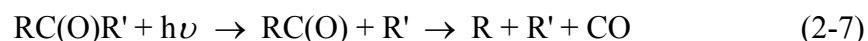
Carbon monoxide is emitted by decaying plant matter exposed to sunlight.^{152,153} The system displays hysteresis and a quadratic dependence of CO production rates on photon flux. Both phenomena are consistent with the build-up of the intermediate CO precursors under high-irradiance conditions. The proposed mechanism involves the photocleavage of the α -glycosidic bonds of the cellulose chain into free radicals, followed by decarbonylation and the formation of non-cyclic hydroxyketones.^{152,153} Thus, cellulose-based organic matter of natural origin undergoes progressive degradative photochemical oxidation into simpler species and releases CO in the process. The shift of the absorption spectra towards the blue is the result of the progressive loss of conjugation in the remaining species.

Carbon monoxide is also produced by photodegradation of dissolved organic matter (DOM) in rain¹⁵⁴ and snow.³⁶ The mechanisms involved are not completely understood, but CO photochemical formation rates were found to be strongly correlated with the concentrations of dissolved organic carbon (DOC), its UV absorbance, and its fluorescence yield.¹³⁴ These observations implicate carbonyl functional groups associated with the relevant chromophores. Formaldehyde is also produced from illuminated snowpacks, but the mechanism of this process probably involves photooxidation, rather than photodecomposition of organic material.²⁸ It has been demonstrated that the photochemical production of CO and carbonyl sulfide OCS from dissolved organic matter in natural waters share a common acyl radical intermediate.¹⁵⁵ Addition of model carbonyl compounds such as acetylacetonate, pyruvate, and glyoxylate enhance the production rates of both species, whereas the addition of cysteine or bisulfide as reduced sulfur-containing substrates increase OCS formation at the expense of CO. Reductive pretreatment of fulvic acid with NaBH₄, which is expected to reduce carbonyl groups, induces a sharp decrease in the photochemical CO production from this surrogate of natural dissolved organic matter.

Dissolved organic matter is degraded by sunlight into a variety of products, such as CO, CO₂, and organic photoproducts that, although smaller in size than the parent species, remain part of DOM pool¹³³ and share some of its properties. Aquatic humic substances are refractory to microbial oxidation, but are the major chromophores in natural waters. Photoproducts become biologically more available than the original material. About 17 low molecular weight species have been identified as photoproducts, among there are C₁-C₃ aldehydes, formate and acetate, glyoxalate, levulinate, malonate,

and pyruvate. The quantum yields for the production of CO and H₂O₂ from DOM photoreactions are about 0.1% near 300 nm and display similar action spectra. The results are nearly independent of the source of natural water.¹⁵⁶ Dissolved iron increases dramatically CO photoproduction, e.g., 90 µg Fe/L increased CO photoproduction eight-fold. A similar effect was found in the photodecomposition of oxalic, glyoxalic and pyruvic acids.¹⁵⁷ Thus, the water-soluble natural organic matter is expected to be photodegraded into simpler, but functionally related species, by sunlight, while being incorporated into atmospheric aerosol, rain, or snow.

The photochemistry of simple carboxylic acids in aqueous solution has been investigated. Processes that lead to CO production via photochemical decarbonylation are well known and involve an excited carbonyl moiety.¹⁵⁸ In one type of these photoprocesses, the so-called Norrish type I mechanism, the α-bond to the carbonyl group is broken, and a pair of free radicals is formed:



Two types of excited states, n-π* or a π-π*, can participate in reaction 2-7, depending on the conditions. The rate constants for Norrish type I reactions are much faster for n-π* states. However, in aqueous solution the reactivity pattern may be reversed due to stabilization of carbonyl non-bonding electrons by water molecules. This is not the only issue that should be taken into account. Other factors, such as the stability of the acyl RC(O) radicals, are also important in condensed media. Unless the acyl radical decomposes, there is always the possibility of reactant formation via cage recombination.

In natural systems, metal chelation to dicarbonyls may substantially affect their photoreactivity via a ligand-to-metal charge transfer mechanism. Actually, the increased production of CO upon addition of ketoacids to natural waters, but not to pure water, implies photosensitization rather than direct photolysis above 300 nm. Studies on direct photolysis of α -ketoacids in pure water have demonstrated that the neutral rather than anionic species are involved. Because most ketoacids have pK_a values lower than about 4, photodecomposition at neutral pH will be inhibited. In addition, the lower enhancement of CO production rates by glyoxylic vs. pyruvic acid addition suggest that enolization of the aldehydic group $-C(O)H$ is also detrimental. At seawater pH, more than 90% of glyoxylate is in the hydrated form, which does not lend itself to CO formation. In many cases it was found that more than one mole of CO_2 was produced in the decarboxylation of α -ketoacids in the presence of oxygen.¹⁵⁹ Bimolecular electron transfer between two molecules of pyruvic acid, or between pyruvic acid and O_2 , has been postulated, and they may be feasible in the concentrated solutions that accrue from solute rejection into the quasi-liquid layer.

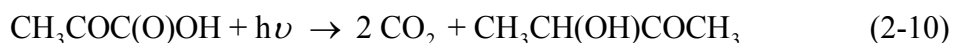
Most ketones lacking γ -H's undergo decarbonylation with nearly unitary quantum yields.¹⁵⁸ Such α -diketones as glyoxal extend their absorption into the red, with strong bands about 430 nm, in addition to the characteristic $C=O$ absorptions at about 280 nm. Their decomposition not only yields CO, but is expected to generate free alkyl radicals as well:



Decomposition quantum yields in solution might be as large as in the gas phase, if the lifetime of the primary HCO radical were very short. Acyl radical decomposition is not an easily reversed process i.e., radical addition to a closed-shell species such as CO has sizable activation energy, rendering cage effects inoperative (see below), while in the gas phase pyruvic acid undergoes quantitative decarboxylation into CO₂ and CH₃CHO: ^{160,161}



with a quantum yield of $\phi_{2.9} = 0.8$ at 366 nm. On the other hand, dimethyltartaric acids are formed in methanol as a solvent. The products of the photoreaction in water are very different. Pyruvic acid in water shows two near-ultraviolet absorption maxima; an n- π^* band with $\lambda_{\text{max}} = 321.2$ nm with a small extinction coefficient ($\epsilon = 11.3 \text{ M}^{-1} \text{ cm}^{-1}$), and a π - π^* band at $\lambda_{\text{max}} = 200.0$ nm ($\epsilon = 2100 \text{ M}^{-1} \text{ cm}^{-1}$).¹⁶⁰ In the past it has been reported that aqueous solutions of pyruvic acid upon ultraviolet irradiation under anoxic conditions evolve carbon dioxide, leaving 3-hydroxy-2-butanone, “acetoin”, as the only organic product remaining in solution:



based on gas chromatography (GC) retention times in which water eluted simultaneously with acetoin.¹⁶⁰ The quantum yield for this process was measured based on ultraviolet absorbance changes before and after irradiation at 366.6 nm: $\phi_{2-10} = 0.79 \pm 0.05$ at 298 K.¹⁶⁰ We have actually extensively restudied the 320 nm band photodecarboxylation of

pyruvic acid in water solutions¹⁶² and found the reaction products (see Chapter 4). Pyruvic acid is photochemically inert in benzene, a solvent unable to donate hydrogens, probably via deactivation of the excited state by the solvent, but in the presence of oxygen undergoes photooxidation into peracetic acid (50%), H₂O₂ (10%), and CH₄ (~20%).¹⁶³ Pyruvate is photochemically unreactive under the same conditions: $\phi < 0.04$.¹⁶⁰ In the presence of hydrogen-donating organic solvents like methanol, pyruvic acid is photoreduced into 2,3-dimethyltartaric acid and at least a 1:1 solvent adduct (2-methyl-2,3-dihydroxypropanoic acid) without significant decarboxylation.¹⁶⁴

The photolysis of aqueous biacetyl, the phototypical α -dicarbonyl, in the presence of O₂ leads to acetic acid, peroxyacetic acid, and hydrogen peroxide.¹⁴⁹ The reaction in aqueous media yields stabilized acetyl radicals, which become hydrated and react with O₂ to produce acetylperoxide radicals. In contrast, the gas-phase photolysis of biacetyl is a source of acetyl radicals and yields CO, H₂, and formaldehyde.¹⁵¹

The photooxidation of organic and inorganic substrates during UV photolysis of nitrite anion in aqueous solutions has been studied by EMR spin trapping (OH radicals by DMPO, NO₂ by aci-nitromethane), and O₂ consumption techniques.¹⁶⁵⁻¹⁶⁸ Since nitrite is the main product of nitrate anion photolysis in water and ice¹⁶⁹ above 300 nm, and the secondary decomposition of nitrite by OH radicals is efficiently inhibited by formate,¹⁷⁰ it is interesting to speculate about the possibility that the photochemically produced OH radicals could drive organic oxidations in ice. NO₂, another product of nitrate anion photolysis, can add to double bonds to initiate the oxidation of unsaturated fatty acids,¹⁷¹ to abstract hydrogen from alkenes,¹⁷² and to oxidize thiols to disulfides; γ -irradiation of ice also produces OH radicals that have been trapped by DMPO.¹⁷³

Photochemical Processes in Ice

The extent to which all the above factors are modified in ice relative to aqueous solutions remains an open field. Solute segregation will in principle shift the hydration equilibrium of aldehydes and ketones to the keto-forms, but the issue whether solutes are really immersed in a quasi-liquid layer down to $-50\text{ }^{\circ}\text{C}$ will strongly qualify such tentative conclusion. Acid-base equilibria may also shift upon freezing.

Ice as an organized medium may influence photochemical reactions by creating a reaction cavity.¹⁷⁴ However, the concept of “reactive cavity” as a time-independent structural constraint imposed by the medium must be qualified in the case of ice, and more so for the environment provided by the quasi-liquid layer. The “effective reaction cavity” will depend on the lifetime of the chromophore excited state and the dynamics of the cavity. The actual geometry of ice cavities may be two- or three-dimensional. The quasi-liquid layer may actually behave as a two-dimensional supercage. In other words, the effective constraints will depend on the solute as well. How easily a medium responds to shape changes or volume demands that occur during the course of a reaction depends on the microviscosity of the medium and the cooperativity of motions involving host and guest molecules. The cavity may be active or passive as well. Ice could interact with polar and H-bonding species. Finally, it should be borne in mind that geometry and polarizability of the excited states are in general different from ground states.

One can investigate the consequences of an enclosure, as provided by ice about a solute, or on unimolecular reactions, such as the photochemical decomposition of an isolated chromophore. This is the so-called cage effect that has been thoroughly studied using unsymmetrical species around the bond being broken, such as substituted

dibenzylketones. The environmental important photochemical decomposition of nitrate at 310 nm in polycrystalline ice as a function of temperature has been recently studied. The quantum yields of NO_2 and NO_2^- formation are similar to their solution values, and their temperature dependence is monotonic above and below the freezing point.^{169,170,175} Moreover, the quantum yield increases, as with temperature, track the fluidity (the reciprocal of viscosity) of water and supercooled water, strongly suggesting that primary photochemical events take place in the quasi-liquid layer and that the photochemically relevant properties of the quasi-liquid layer correspond to fluid water.

Ice itself can undergo photochemical decomposition into H and OH radicals. The long-wavelength cutoff of ice is shifted to the blue ($\lambda < 190$ nm) relative to that of helium-purged liquid water ($\lambda < 200$ nm). O_2 -saturated water absorbs above 200 nm, with an extinction coefficient of about 0.03 cm^{-1} at 210 nm, 298 K.¹⁷⁶ Langford et al. showed that crystalline, polycrystalline, and amorphous ices irradiated at 220 and 260 nm, i.e., longer than the dissociation threshold at 242 nm in the gas phase, displaying luminescence that has been ascribed to Herzberg band emissions from O_2^* at 340 nm, and from spin-forbidden $^4\Sigma \rightarrow X^2\Pi$ transition of OH radicals.¹⁷⁷ Thermodynamically, dissociation of H_2O in ice can occur for wavelengths as long as 270 nm, due to the stabilization of the OH photoproducts in the ice lattice. The implication is that radiation close to the atmospheric ozone cutoff can induce excited state photochemistry in ice.

Assuming that Cerenkov radiation is absorbed exclusively by organic ice dopants, which in turn undergo decarbonylation with nearly unitary quantum efficiency, it has been estimated a production of about 4×10^{11} CO molecules cm^{-3} during 1000 years (see above). From the ~ 100 ppbv CO excess found in 1000 year old Greenland ice cores with

respect to data obtained in the Antarctic,³⁵ which are simultaneous with 20 ppmv CO₂ excesses corresponding to about 0.08 μmol/Kg,³⁴ Colussi and Hoffmann¹⁷⁸ obtained a CO concentration excess of 2×10^{11} CO molecules cm⁻³, i.e., in fair agreement with their estimates. In other words, given the uncertainties associated with some of these assumptions, photochemistry in deep ice cores driven by Cerenkov radiation could account for a substantial fraction of excess CO and CO₂.

References

- 1- Legrand, M.; Mayewski, P. *Rev. Geophys.* **1997**, *35*, 219.
- 2- Anklin, M.; Bales, R.; Mosley-Thompson, E.; Steffen, K. *J. Geophys. Res.* **1998**, *103*, 28775.
- 3- Bales, R. C.; Wolff, E. W. *EOS Trans.* **1995**, *76*, 482.
- 4- Laj, P.; Palais, J. M.; Sigurdsson, H. *Atmos. Environ.* **1992**, *26*, 2627.
- 5- King, M.; Simpson, W. *J. Geophys. Res.* **2001**, *106*, 12499.
- 6- Gerland, S.; Winther, J. G. et al. *Hydrological Processes* **1999**, *13*, 2331.
- 7- Mellor, M. J. *Glaciol.* **1977**, *19*, 15.
- 8- Mulvaney, R.; Wagenbach, D.; Wolff, E. W. *J. Geophys. Res.* **1998**, *103*, 11021.
- 9- Mulvaney, R.; Wolff, W. *J. Geophys. Res.* **1993**, *98*, 5213.
- 10- Rothlisberger, R.; Hutterli, M. A.; Sommer, S.; Wolff, E. W.; Mulvaney, R. *J. Geophys. Res.* **2000**, *105*, 20565.
- 11- Wolff, E. W.; Hall, J. S.; Mulvaney, R.; Pasteur, E. C.; Wagenbach, D.; Legrand, M. *J. Geophys. Res.* **1998**, *103*, 11057.
- 12- Thomas, D. N.; Lara, R. J.; Eicken, H.; Kattner, G.; Skoog, A. *Polar Biology* **1995**, *15*, 477.
- 13- Davis, D.; Nowak, J.; Chen, G.; Buhr, M.; Arimoto, R.; Hogan, A.; Eisele, F.; Mauldin, L.; Tanner, D.; Shetter, R.; Lefer, B.; McMurry, P. *Geophys. Res. Lett.* **2001**, *28*, 3625.
- 14- Weller, R.; Minikin, A.; Konig-Langlo, G.; Schrems, O.; Jones, A. E.; Wolff, E. W.; Anderson, P. S. *Geophys. Res. Lett.* **1999**, *26*, 2853.
- 15- Trodahl, H. J.; Buckley, R. G. *Science* **1989**, *245*, 194.

- 16- Couch, T. L.; Sumner, A. L.; Dassau, T. M.; Shepson, P. B.; Honrath, R. E.
Geophys. Res. Lett. **2000**, *27*, 2241.
- 17- Honrath, R.; Guo, S.; Peterson, M.; Dziobak, M.; Dibb, J.; Arsenault, M.
J. Geophys. Res. **2000**, *105*, 24183.
- 18- Honrath, R. E.; Peterson, M. C.; Dziobak, M. P.; Green, S.; Dibb, J. E.; Arsenault,
M. A. *Geophys. Res. Lett.* **2000a**, *27*, 2237.
- 19- Honrath, R. E.; Peterson, M. C.; Guo, S.; Dibb, J. E.; Shepson, P. B.; Campbell, B.
Geophys. Res. Lett. **1999**, *26*, 695.
- 20- Mayewski, P. A.; Lyons, W. B.; Spencer, M. J.; Twickler, M.; Dansgaard, W.;
Koci, B.; Davidson, C. I.; Honrath, R. E. *Science* **1986**, *232*, 975.
- 21- Peterson, M.; Honrath, R. *J. Geophys. Res.* **1999**, *104*, 11695.
- 22- Dibb, J. E.; Talbot, R. W.; Munger, J. W.; Jacob, D. J.; Fan, S. M. *J. Geophys. Res.*
1998, *103*, 3475.
- 23- Munger, J. W.; Jacob, D. et al. *J. Geophys. Res.* **1999**, *104*, 13721.
- 24- Jones, A. E.; Weller, R.; Minikin, A.; Wolff, E. W.; Stuges, W. T.; McIntyre, H. P.;
Leonard, S. R.; Schrems, O.; Bauguitte, S. *J. Geophys. Res.* **1999**, *104*, 21355.
- 25- Jacobi, H.; Weller, R.; Jones, A.; Anderson, P.; Schrems, O. *Atmos. Environ.* **2000**,
34, 5235.
- 26- Jones, A. E.; Weller, R.; Wolff, E. W.; Jacobi, H.-W. *Geophys. Res. Lett.* **2000**, *27*,
345.
- 27- Bottenheim, J. W.; Barrie, L. A.; Atlas, E. *J. Atmos. Chem.* **1993**, *17*, 15.
- 28- Sumner, A. L.; Shepson, P. B. *Nature* **1999**, *398*, 230.
- 29- Ridley, B.; Walega, J.; Montzka, D.; Grahek, F.; Atlas, E.; Flocke, F.; Stroud, V.;

- Deary, J.; Gallant, A.; Boudries, H.; Bottenheim, J.; Anlauf, K.; Worthy, D.; Sumner, A. I.; Splawn, B.; Shepson, P. *J. Atmos. Chem.* **2000**, *36*, 1.
- 30- Michalowski, B.; Francisco, J.; Li, S.; Barrie, L.; Bottenheim, J.; Shepson, P. *J. Geophys. Res.* **2000**, *105*, 15131.
- 31- Houdier, S.; Perrier, S.; Domine, F.; Cobanes, A.; Legagneux, L.; Grannas, A. M.; Guimbaud, C.; Shepson, P. B.; Boudries, H.; Bottenheim, J. "Snow-Phase Acetaldehyde (CH₃CHO) and Acetone (CH₃)₂CO in the Arctic Snowpack"; AGU, 2000, San Francisco, California.
- 32- Zhou, X. L.; Beine, H. J.; Honrath, R. E.; Fuentes, J. D.; Simpson, W.; Shepson, P. B.; Bottenheim, J. W. *Geophys. Res. Lett.* **2001**, *28*, 4087.
- 33- Peterson, M. C.; Honrath, R. E. *Geophys. Res. Lett.* **2001**, *28*, 511.
- 34- Tschumi, J.; Stauffer, B. *J. Glaciol.* **2000**, *46*, 45.
- 35- Haan, D.; Raynaud, D. *Tellus* **1998**, *50 B*, 253.
- 36- Haan, D.; Zuo, Y.; Gros, V.; Brenninkmeijer, C. *J. Atmos. Chem.* **2001**, *40*, 217.
- 37- Jackson, A. *Critical Reviews in Environ. Sci. Technol.* **1999**, *29*, 175.
- 38- Sigg, A.; Neftle, A. *Nature* **1991**, *351*, 557.
- 39- Sigg, A.; Staffelbach, T.; Neftel, A. *J. Atmos. Chem.* **1992**, *14*, 223.
- 40- Gayley, R. I.; Ram, M. *J. Geophys. Res.* **1985**, *90*, 12921.
- 41- Lin, S. S.; Gurol, M. *Environ. Sci. Technol.* **1998**, *32*, 1417.
- 42- Nikolaev, P. V.; Ignatov, V. A. *J. Appl. Chem. USSR* **1983**, *46*, 5.
- 43- Suresh, S. J.; Naik, V. M. *J. Chem. Phys.* **2000**, *113*, 9727.
- 44- Rick, S. W. *J. Chem. Phys.* **2001**, *114*, 2276.
- 45- Cowin, J. P.; Tsekouras, A. A.; Iedema, M. J.; Wu, K.; Ellison, G. B. *Nature* **1999**,

- 398, 405.
- 46- Onsager, L.; Runnels, L. K. *J. Chem. Phys.* **1969**, *50*, 1089.
- 47- Park, S.-C.; Maeng, K.-W.; Pradeep, T.; H., K. *Angew. Chem. Int. Ed.* **2001**, *40*, 1497.
- 48- Park, S.; Pradeep, T.; Kang, H. *J. Chem. Phys.* **2000**, *113*, 9373.
- 49- Hynes, R.; Mossinger, J.; Cox, R. *Geophys. Res. Lett.* **2001**, *28*, 2827.
- 50- Kallay, N.; Cakara, D. *J. Coll. Interfac. Sci.* **2000**, *232*, 81.
- 51- Glenn, D. F.; Ingram, J. C. *J. Electrochem. Soc.* **1994**, *141*, L113.
- 52- Doe, H.; Kobayashi, T.; Sawada, H. *J. Electroanal. Chem.* **1995**, *383*, 53.
- 53- Drzymala, J.; Sadowski, Z.; Holysz, L.; Chibowski, E. *J. Coll. Interfac. Sci.* **1999**, *220*, 229.
- 54- Hobbs, P. V. *Ice Physics*; Clarendon Press: Oxford, 1974.
- 55- Wettlaufer, J. S. *Phil. Trans. Royal Soc. London, Series A* **1999**, *357*, 3403.
- 56- Olander, D. S.; Rice, S. A. *Proc. Natl. Acad. Sci. U. S. A.* **1972**, *69*, 98.
- 57- Gertner, B. J.; Hynes, J. T. *Science* **1996**, *271*, 1563.
- 58- Zuberi, B.; Bertram, A.; Koop, T.; Molina, L.; Molina, M. *J. Phys. Chem. A* **2001**, *105*, 6458.
- 59- Trakhtenberg, S.; Naaman, R.; Cohen, S. R.; Benjamin, I. *J. Phys. Chem. B* **1997**, *101*, 5172.
- 60- Chaabouni, H.; Schriver-Mazzuoli, L.; Schriver, A. *Low Temp. Phys.* **2000**, *26*, 712.
- 61- Chaabouni, H.; Schriver-Mazzuoli, L.; Schriver, A. *J. Phys. Chem. A* **2000**, *104*, 6962.

- 62- Miranda, P. B.; Xu, L.; Shen, Y. R.; Salmeron, M. *Phys. Rev. Lett.* **1998**, *81*, 5876.
- 63- Bluhm, H.; Inoue, T.; Salmeron, M. *Abstracts of Papers of the American Chemical Society* **1999**, *217*, U633.
- 64- Bluhm, H.; Inoue, T.; Salmeron, M. *Surf. Sci.* **2000**, *462*, L599.
- 65- Bluhm, H.; Inoue, T.; Salmeron, M. *Phys. Rev. B* **2000**, *61*, 7760.
- 66- Bluhm, H.; Salmeron, M. *J. Chem. Phys.* **1999**, *111*, 6947.
- 67- Salmeron, M.; Bluhm, H. *Surf. Rev. and Lett.* **1999**, *6*, 1275.
- 68- Su, X.; Lianos, L.; Shen, Y. R.; Somorjai, G. *Phys. Rev. Lett.* **1998**, *80*, 1533.
- 69- Delzeit, L.; Devlin, M.; Rowland, B.; Devlin, J.; Buch, V. *J. Phys. Chem.* **1996**, *100*, 10076.
- 70- Wilen, L. A.; Wettlaufer, J. S.; Elbaum, M.; Schick, M. *Phys. Rev. B* **1995**, *52*, 12426.
- 71- Israelachvili, J. *Intermolecular and Surface Forces*; Academic Press: San Diego, CA, 1992.
- 72- Li, Y. Q.; Davidovits, P.; Shi, Q.; Jayne, J. T.; Kolb, C. E.; Worsnop, D. R. *J. Phys. Chem. A* **2001**.
- 73- Knight, C. *J. Geophys. Res.* **1996**, *101*, 12921.
- 74- Baker, M. B.; Dash, J. G. *Geophys. Res. Lett.* **1996**, *101*, 12929.
- 75- Doppenschmidt, A.; Butt, H.-J. *Langmuir* **2000**, *16*, 6709.
- 76- Doppenschmidt, A.; Kappl, M.; Butt, H.-J. *J. Phys. Chem. B* **1998**, *102*, 7813.
- 77- Dash, J. G.; Fu, H. Y.; Wettlaufer, J. S. *Reports on Progress in Physics* **1995**, *58*, 115.
- 78- Wettlaufer, J. S. *Phys. Rev. Lett.* **1999**, *82*, 2516.

- 79- Wettlaufer, J. S.; Dash, J. G. *Scientific American* **2000**, 282, 50.
- 80- Mantz, Y.; Geiger, F.; Molina, L.; Molina, M.; Trout, B. *J. Chem. Phys.* **2000**, 113, 10733.
- 81- Huthwelker, T.; Lamb, D.; Baker, M.; Swanson, B.; Peter, T. *J. Coll. Interfac. Sci.* **2001**, 238, 147.
- 82- Cullen, D.; Baker, I. *J. Glaciol.* **2000**, 46, 703.
- 83- Bolton, K.; Pettersson, J. B. C. *J. Phys. Chem. B* **2000**, 104, 1590.
- 84- Pincock, R. E. *Acc. Chem. Res.* **1969**, 2, 97.
- 85- van der Ham, F.; Witkamp, G. J.; de Graauw, J.; van Rosmalen, G. M. *J. Cryst. Growth* **1999**, 198/199, 744.
- 86- Killawee, J. A.; Fairchild, I. J.; Tison, J. L.; Janssens, L.; Lorrain, R. *Geochimica et Cosmochimica Acta* **1998**, 62, 3637.
- 87- Gross, G. W.; Gutjahr, A.; Caylor, K. *Journal de Physique* **1987**, 48, 527.
- 88- Gross, G.; Svec, R. *J. Phys. Chem. B* **1997**, 101, 6282.
- 89- Conklin, M.; Bales, R. C. *J. Geophys. Res.* **1993**, 98, 16851.
- 90- Choi, J.; Conklin, M. H.; Bales, R. C.; Sommerfeld, R. A. *Atmos. Environ.* **2000**, 34, 793.
- 91- Oremp, M. W.; Adamson, A. R. *J. Coll. Interf. Sci.* **1969**, 31, 278.
- 92- Kawamura, K.; Yokoyama, K.; Fujii, Y.; Watanabe, O. *J. Geophys. Res.* **2001**, 106, 1331.
- 93- Kawamura, K.; Suzuki, I.; Fujii, Y.; Watanabe, O. *Geophys. Res. Lett.* **1996**, 23, 2665.
- 94- Thibert, E.; Domine, F. *J. Phys. Chem. B* **1998**, 102, 4432.

- 95- Nye, J. F. *J. Glaciol.* **1989**, 35, 17.
- 96- Potts, W. T. W.; Oates, K.; Wolff, E. W.; Mulvaney, R. *Scanning Microscopy* **1992**, 6, 295.
- 97- Devlin, J.; Uras, N.; Rahman, M.; Buch, V. *Israel J. Chem.* **1999**, 39, 261.
- 98- Livingston, F.; Smith, J.; George, S. *Anal. Chem.* **2000**, 72, 5590.
- 99- Livingston, F.; George, S. *J. Phys. Chem. A* **2001**, 105, 5155.
- 100- Sommerfeld, R. A.; Knight, C. A.; Laird, S. K. *Geophys. Res. Lett.* **1998**, 25, 935.
- 101- Laird, S.; Buttry, D.; Sommerfeld, R. *Geophys. Res. Lett.* **1999**, 26, 699.
- 102- Domine, F.; Thibert, E. *Geophys. Res. Lett.* **1998**, 25, 4389.
- 103- Nakamura, K.; Masayoshi, N.; Ageta, Y.; Goto-Azuma, K.; Kamiyama, K. Post-depositional loss of nitrate in surface snow layers of the Antarctic ice sheet. In *The Physics of Ice Core Records*; Hondoh, T., Ed.; Hokkaido University Press: Sapporo, 2000; pp. 214.
- 104- Fabre, A.; Barnola, J. M.; Arnaud, L.; Chapellaz. *Geophys. Res. Lett.* **2000**, 27, 557.
- 105- Kiovsky, T. E.; Pincock, R. E. *J. Chem. Ed.* **1966**, 43, 361.
- 106- Sola, M. I.; Corti, H. R. *Anal. Assoc. Quim. Arg.* **1993**, 81, 483.
- 107- Takenaka, N.; Diamon, T.; Ueda, A.; Sato, K.; Kitano, M.; Bandow, H.; Maeda, Y. *J. Atmos. Chem.* **1998**, 29, 135.
- 108- Takenaka, N.; Ueda, A.; Daimon, T.; Bandow, H.; Dohmaru, T.; Maeda, Y. *J. Phys. Chem.* **1996**, 100, 13874.
- 109- Takenaka, N.; Ueda, A.; Maeda, Y. *Nature* **1992**, 358, 736.
- 110- Honda, K. "Acceleration of sulfurous acid oxidation by freezing of aqueous

- solution”; Nippon Kagaku Kaishi, 2001.
- 111- Betterton, E. A.; Anderson, D. J. “Autooxidation of N(III), S(IV) and other species in Frozen Solution - Possible Pathway for Enhanced Chemical Transformation in Freezing Systems”; ACS, 2001, San Diego, California.
- 112- Horne, R. A. *J. Inorg. Nucl. Chem.* **1963**, 25, 1139.
- 113- Sinner, T.; Hoffmann, P.; Knapp, C. P.; Ortner, H. M. *Fresenius J. Anal. Chem.* **1994**, 349, 334.
- 114- O'Driscoll, P.; Lang, K.; Minogue, N.; Sondeau, J. *J. Phys. Chem. A* **2006**, 110.
- 115- Finnegan, W. G.; Pitter, R. L. *Atmos. Environ.* **1991**, 25A, 2912.
- 116- Finnegan, W.; Pitter, R. *J. Coll. Interfac. Sci.* **1997**, 189, 322.
- 117- Finnegan, W.; Pitter, R.; Hinsvark, B. *J. Coll. Interfac. Sci.* **2001**, 242, 373.
- 118- Finnegan, W. G.; Pitter, R. L.; Young, L. G. *Atmos. Environ.* **1991**, 25, 2531.
- 119- Workman, E. J.; Reynolds, S. E. *Phys. Rev.* **1950**, 78, 1950.
- 120- Bronshteyn, V. L.; Chernov, A. A. *J. Crystal Growth* **1991**, 112, 129.
- 121- Shibkov, A.; Golovin, Y.; Zheltov, M.; Korolev, A. *Crystallography Reports* **2001**, 46, 144.
- 122- Lodge, J. P.; Baker, M. L.; Pierrard, J. M. *J. Chem. Phys.* **1956**, 24, 716.
- 123- Gross, G. W.; McKee, C.; Wu, C.-H. *J. Chem. Phys.* **1975**, 62, 3080.
- 124- Hemley, R. *Ann. Rev. Phys. Chem.* **2000**, 51, 763.
- 125- *Physics of Ice Core Records*; Hondoh, T., Ed.; Hokkaido University Press: Sapporo, Japan, 2000.
- 126- Andres, E.; Askebjerg, P.; Bai, X. et al. *Nature* **2001**, 410, 441.
- 127- Jelley, J. V. *Cerenkov Radiation*; Pergamon: New York, 1958.

- 128- Thompson, M. G. Energetic muons. In *Cosmic Rays at Ground Level*; Wolfendale, A. W., Ed.; The Institute of Physics: London, 1973; pp. 17.
- 129- Beukers, R.; Ijlstra, J.; Berends, W. *Rec. Trav. Chim.* **1959**, *77*, 729.
- 130- Glendinning, J. H. G.; Morris, E. M. *Hydrological Processes* **1999**, *13*, 1761.
- 131- Franchy, R. *Rep. Prog. Phys.* **1998**, *61*, 691.
- 132- Perovich, D. K.; Govoni, J. W. *Geophys. Res. Lett.* **1991**, *18*, 1233.
- 133- Moran, M. A.; Zepp, R. G. *Limnol. and Oceanogr.* **1997**, *42*, 1307.
- 134- Zuo, Y. G.; Jones, R. D. *Water Research* **1997**, *31*, 850.
- 135- Belzile, C.; Johannessen, S.; Gosselin, M.; Demers, S.; Miller, W. *Limn. and Oceanogr.* **2000**, *45*, 1265.
- 136- Szent-Gyorgyi, A. *Bioenergetics*; Academic: New York, 1957.
- 137- Leigh, J. S.; Reed, G. H. *J. Phys. Chem.* **1971**, *75*, 1202.
- 138- Graham, J.; Roberts, J. *J. Phys. Chem. B* **2000**, *104*, 978.
- 139- Baboukas, E. D.; Kanakidou, M.; Mihalopoulos, N. *J. Geophys. Res.* **2000**, *105*, 14459.
- 140- Yu, S. C. *Atmos. Res.* **2000**, *53*, 185.
- 141- Legrand, M.; Deangelis, M. *J. Geophys. Res.* **1995**, *100*, 1445.
- 142- Krivacsy, Z.; Kiss, G.; Varga, B.; Galambos, I.; Sarvari, Z.; Gelencser, A.; Molnar, A.; Fuzzi, S.; Facchini, M.; Zappoli, S.; Andracchio, A.; Alsberg, T.; Hansson, H. C.; Persson, L. *Atmos. Environ.* **2000**, *34*, 4273.
- 143- Kawamura, K.; Yokoyama, K.; Fujii, Y.; Watanabe, O. *Geophys. Res. Lett.* **1999**, *26*, 871.
- 144- Sempere, R.; Kawamura, K. *Atmos. Environ.* **1996**, *30*, 1609.

- 145- Bailey, P. S. "Ozone reactions with organic compounds"; 161st meeting of the American Chemical Society, 1972, Los Angeles, Calif., March 29–30, 1971.
- 146- Kiss, G.; Varga, B.; Gelencser, A.; Krivacsy, Z.; Molnar, A.; Alsberg, T.; Persson, L.; Hansson, H. C.; Facchini, M. C. *Atmos. Environ.* **2001**, *35*, 2193.
- 147- Fuzzi, S.; Decesari, S.; Facchini, M. C.; Matta, E.; Mircea, M.; Tagliavini, E. *Geophys. Res. Lett.* **2001**, *28*, 4079.
- 148- Xu, H.; Wentworth, P. J.; Howell, N. W.; Joens, J. A. *Spectrochim. Acta* **1993**, *49A*, 1171.
- 149- Faust, B.; Powell, K.; Rao, C.; Anastasio, C. *Atmos. Environ.* **1997**, *31*, 497.
- 150- Steenken, S.; Sprague, E. D.; Schulte-Frohlinde, D. *Photochem. Photobiol.* **1975**, *22*, 19.
- 151- Finlayson-Pitts, B. J.; Pitts, J. N. *Atmospheric Chemistry*; Wiley: New York, 1986.
- 152- Schade, G. W.; Crutzen, P. J. *Tellus* **1999**, *51 B*, 909.
- 153- Schade, G. W.; Hofmann, R. M.; Crutzen, P. J. *Tellus* **1999**, *51 B*, 889.
- 154- Zuo, Y.; Jones, R. D. *Geophys. Res. Lett.* **1996**, *23*, 2769.
- 155- Pos, W. H.; Riemer, D. D.; Zika, R. G. *Marine Chemistry* **1998**, *62*, 89.
- 156- Valentine, E. L.; Zepp, R. G. *Environ. Sci. Technol.* **1993**, *27*, 409.
- 157- Zuo, Y. G.; Hoigne, J. *Atmos. Environ.* **1994**, *28*, 1231.
- 158- Kagan, J. *Organic Photochemistry, Principles and Applications*; Academic Press: San Diego, CA, 1993; chapter 4.
- 159- Davidson, R. S.; Goodwin, D. *Tetrahedron Letters* **1980**, *21*, 4943.
- 160- Leermakers, P. A.; Vesley, G. F. *J. Am. Chem. Soc.* **1963**, *85*, 3776.
- 161- Vesley, G. F.; Leermakers, P. A. *J. Phys. Chem.* **1964**, *68*, 2364.

- 162- Guzmán, M. I.; Colussi, A. J.; Hoffmann, M. R. *J. Phys. Chem. A* **2006**, *110*, 3619.
- 163- Sawaki, Y.; Ogata, Y. *J. Am. Chem. Soc.* **1981**, *103*, 6455.
- 164- Barton, D. H. R.; P., D.; Shafiq, M. *J. Chem. Soc.* **1958**, 140.
- 165- Bilski, P.; Chignell, C. F.; Szychlinski, J.; Borowski, A.; Olewsky, E.; Reszka, K. *J. Am. Chem. Soc.* **1992**, *114*, 549.
- 166- Zuo, Y.; Deng, Y. *Chemosphere* **1998**, *36*, 181.
- 167- Arakaki, T.; Miyake, T.; Hirakawa, T.; Sakugawa, H. *Environ. Sci. Technol.* **1999**, *33*, 2561.
- 168- Pace, M. D.; Carmichael, A. J. *J. Phys. Chem. A* **1997**, *101*, 1848.
- 169- Dubowski, Y.; Colussi, A. J.; Hoffmann, M. R. *J. Phys. Chem. A* **2001**, *105*, 4928.
- 170- Dubowski, Y.; Colussi, A. J.; Hoffmann, M. R. *J. Phys. Chem. A* **2002**.
- 171- Pryor, W. A.; Lightsey, J. W. *Science* **1981**, *214*, 435.
- 172- Pryor, W. A.; Lightsey, J. W.; Church, D. F. *J. Am. Chem. Soc.* **1982**, *104*, 6685.
- 173- Yoshioka, H.; Hasegawa, K. *Biosci. Biotechnol. Biochem.* **1996**, *60*, 1971.
- 174- Ramamurthy, V.; Weiss, R. G.; Hammond, G. S. A model for the influence of organized media on photochemical reactions. In *Advances in Photochemistry*; Volman, D. H. et al. Eds.; J. Wiley: New York, 1993; Vol. 18; pp. 67.
- 175- Dubowski, Y.; Hoffmann, M. R. *Geophys. Res. Lett.* **2000**, *27*, 3321.
- 176- Ghormley, J. A.; Hochanadel, C. J. *The J. Phys. Chem.* **1971**, *75*, 40.
- 177- Langford, V.; McKinley, A.; Quickenden, T. *Acc. Chem. Res.* **2000**, *33*, 665.
- 178- Colussi, A. J.; Hoffmann, M. R. *Geophys. Res. Lett.* **2003**, *30*, 1195.